

Synthesis of Dumbbell-Shaped Au–Ag Core–Shell Nanorods by Seed-Mediated Growth under Alkaline Conditions

Chih-Ching Huang, Zusing Yang, and Huan-Tsung Chang*

Department of Chemistry, National Taiwan University, Taipei, Taiwan

Received May 15, 2004

We report a simple synthesis of Au–Ag core–shell nanorods (NRs) under alkaline conditions (pH 8.0–10.0) from silver and ascorbate ions using gold nanorods (GNRs) as the seeds. The silver ions that are reduced by the ascorbate ions become deposited on the surfaces of the GNRs to form differently dumbbell-shaped Au–Ag core–shell NRs and nanoparticles, depending on the pH and the concentration of silver ions. The longitudinal plasmon absorbance bands of the Au–Ag core–shell NRs are stronger and appear at shorter wavelengths than those for the original GNRs. We confirmed the formation of Au–Ag core–shell NRs by both energy-dispersive X-ray spectrometry and inductively coupled plasma mass spectrometry measurements, which indicate that the $^{109}\text{Ag}/^{197}\text{Au}$ ratios are 0.046, 0.085, and 0.097 at pH 8.0, 9.0, and 10.0, respectively. The transmission electron microscopy measurements show that the Au–Ag core–shell NRs are monodispersed (>90%).

Nanoparticles (NPs) exhibit significantly different properties relative to those of their corresponding bulk materials and, as such, are of interest for applications in catalysis, electronics, and optics.^{1–9} Gold nanoparticles (GNPs) can be used as sensors because of the size and shape dependence of their optical properties and the ease by which their surfaces can be modified using biological molecules, such as proteins and DNA, mainly through Au–S bonding.⁶ Spherical GNPs can be synthesized readily by the chemical reduction of gold salts;^{10,11} anisotropic GNPs, such as gold nanorods (GNRs), can be prepared by a variety of methods, such as templating,¹² photochemistry,¹³ seeding,¹⁴ and electrochemistry.¹⁵ The properties of the surfactants^{13–15,16} and organic solvents,^{14,15} as well as the concentration of the seeds,¹⁷ are

important parameters for controlling the aspect ratios (length:width) of the GNRs. In addition, the concentration of silver ions is also critical to the control of the aspect ratio of GNRs prepared by photochemical means.^{13b,14d}

Core–shell bimetallic nanoparticles exhibiting characteristic electronic, optical, and catalytic properties, which are different from those of their individual constituent metals, are of considerable interest in basic and applied science.^{18,19} In this paper, we describe an easy approach to the synthesis of differently shaped Au–Ag core–shell nanorods (NRs) from silver ions and ascorbic acid, under alkaline conditions, using GNRs (aspect ratio = 3.92) as seeds. At low pH, ascorbic acid (the values of $\text{p}K_{\text{a}1}$ and $\text{p}K_{\text{a}2}$ are 4.10 and 11.79, respectively), which is incapable of reducing silver ions, is the major species; the fraction of monoanionic ascorbate species, which are capable of reducing silver ions, increases as the value of the pH increases.^{13b,14d,20a,b} Thus, we expected that the deposition of reduced silver atoms onto the surface of the GNRs occurs at high pH. To test our hypothesis, we conducted the following reactions in 200 mM glycine buffers (pH > 7.0). The GNR seeds were prepared using a seeding method according to a literature procedure;^{14d} they were used directly without any further purification. Four aliquots of as-prepared GNR solutions (pH 3.0; 0.5 mL) containing 0.097 mM silver ions and 0.53 mM ascorbic acid were mixed separately with 500 mM glycine buffers (pH 7.0, 8.0, 9.0, and 10.0; 0.4 mL); these mixtures were diluted with water to give final volumes of 2.0 mL. The solutions were then incubated at room temperature for up to 6 h. During the course of the reaction, the color of the solution at pH 7.0 (rose) remained the same while the other three solutions changed to different degrees of

* To whom correspondence may be addressed. Tel./fax: 011-886-2-23621963. E-mail: changht@ntu.edu.tw

- (1) Eychmuller, A. *J. Phys. Chem. B* **2000**, *104*, 6514–6528.
- (2) El-Sayed, M. A. *Acc. Chem. Res.* **2001**, *34*, 257–264.
- (3) Gambardella, P.; Rusponi, S.; Veronese, M.; Dhesi, S. S.; Grazioli, C.; Dallmeyer, A.; Cabria, I.; Zeller, R.; Dederichs, P. H.; Kern, K.; Carbon, C.; Brune, H. *Science* **2003**, *300*, 1130–1133.
- (4) Bell, A. T. *Science* **2003**, *299*, 1688–1691.
- (5) Cui, Y.; Wei, Q.; Park, H.; Lieber, C. M. *Science* **2001**, *293*, 1289–1292.
- (6) Storhoff, J. J.; Lazaridis, A. A.; Mucic, R. C.; Mirkin, C. A.; Letsinger, R. L.; Schatz, G. C. *J. Am. Chem. Soc.* **2000**, *122*, 4640–4650.
- (7) Mulvaney, P. *Langmuir* **1996**, *12*, 788–800.
- (8) Kelly, K. L.; Coronado, E.; Zhao, L. L.; Schatz, G. C. *J. Phys. Chem. B* **2003**, *107*, 668–677.
- (9) Link, S.; Mohamed, M. B.; El-Sayed, M. A. *J. Phys. Chem. B* **1999**, *103*, 3073–3077.
- (10) Turkevich, J.; Stevenson, P. C.; Hillier, J. *Discuss. Faraday Soc.* **1951**, *11*, 55–75.
- (11) Frens, G. *Nat. Phys. Sci.* **1973**, *241*, 20–22.
- (12) (a) van der Zande, B. M. I.; Böhmer, M. R.; Fokink, L. G. J.; Schönenberger, C. *J. Phys. Chem. B* **1997**, *101*, 852–854. (b) Nicewarner-Peña, S. R.; Freeman, R. G.; Reiss, B. D.; He, L.; Peña, D. J.; Walton, I. D.; Cromer, R.; Keating, C. D.; Natan, M. J. *Science* **2001**, *294*, 137–141.
- (13) (a) Esumi, K.; Matsuhisa, K.; Torigoe, K. *Langmuir* **1995**, *11*, 3285–3287. (b) Kim, F.; Song, J. H.; Yang, P. *J. Am. Chem. Soc.* **2002**, *124*, 14316–14317.
- (14) (a) Murphy, C. J.; Jana, N. R. *Adv. Mater.* **2002**, *14*, 80–82. (b) Busbee, B. D.; Obare, S. O.; Murphy, C. J. *Adv. Mater.* **2003**, *15*, 414–416. (c) Taub, N.; Krichevski, O.; Markovich, G. *J. Phys. Chem. B* **2003**, *107*, 11579–11582. (d) Nikoobakht, B.; El-Sayed, M. A. *Chem. Mater.* **2003**, *15*, 1957–1962.
- (15) (a) Yu, Y.-Y.; Chang, S.-S.; Lee, C.-L.; Wang, C. R. C. *J. Phys. Chem. B* **1997**, *101*, 6661–6664. (b) Chang, S.-S.; Shih, C.-W.; Chen, C.-D.; Lai, W.-C.; Wang, C. R. C. *Langmuir* **1999**, *15*, 701–709.

(16) Gao, J.; Bender, C. M.; Murphy, C. J. *Langmuir* **2003**, *19*, 9065–9070.

(17) Jana, N. R.; Gearheart, L.; Murphy, C. J. *J. Phys. Chem. B* **2001**, *105*, 4065–4067.

(18) Henglein, A. *J. Phys. Chem. B* **2000**, *104*, 2201–2203.

(19) Hodak, J. H.; Henglein, A.; Hartland, G. V. *J. Phys. Chem. B* **2000**, *104*, 5053–5055.

(20) (a) Pal, T.; De, S.; Jana, N. R.; Pradhan, N.; Mandal, R.; Pal, A.; Beezer, A. E.; Mitchell, J. C. *Langmuir* **1998**, *14*, 4724–4730. (b) Hodak, J. H.; Henglein, A.; Giersig, M.; Hartland, G. V. *J. Phys. Chem. B* **2000**, *104*, 11708–11718. (c) Liu, M.; Guyot-Sionnest, P. *J. Phys. Chem. B* **2004**, *108*, 5882–5888.

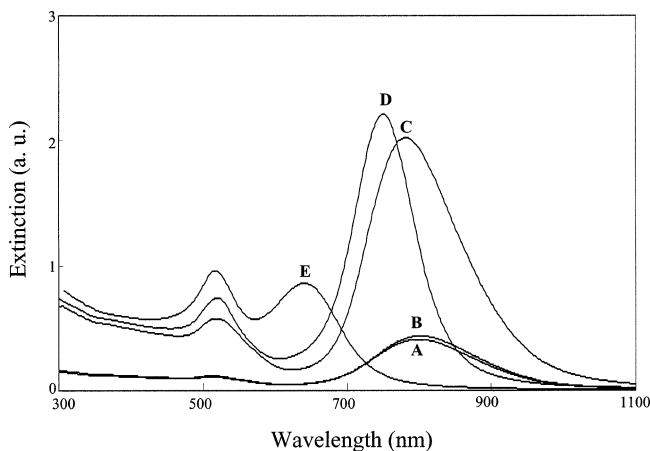


Figure 1. Surface plasmon absorption spectra for (A), the initial GNRs at pH 3.0, and for the GNR in 100 mM glycine solutions containing 0.097 mM silver ions and 0.53 mM ascorbic acid at (B) pH 7.0, (C) pH 8.0, (D) pH 9.0, and (E) pH 10.0.

magenta. In comparison, the color of the solutions did not change in the absence of ascorbate ions. We note that we did not observe AgCl precipitates since silver ions form complexes with glycine. Thus, the solutions were used for UV-vis absorption measurements. For transmission electron microscopy (TEM) measurements, the solutions were subject to centrifugation (12000 rpm for 30 min) to remove excess amounts of CTAB.

As Figure 1 indicates, the UV-vis spectra of the solution at pH 7.0 and the original GNR solution are similar, whereas the longitudinal plasmon absorption bands of the other three solutions undergo blue shifts. The magnitude of the blue shift increases with increasing values of pH in the range from 8.0 to 10.0, which suggests the formation of differently shaped products. Our hypothesis is further confirmed by the TEM images depicted in Figure 2A–D. The TEM intensity contrast suggests the formation

of Au–Ag core–shell NRs, in which the bright parts show the distribution of silver.^{20b,21} The unique shapes of each set of NRs obtained at different values of pH highlight the usefulness of this method for preparing high-quality Au–Ag core–shell NRs. The formation of the Au–Ag core–shell NRs occurs as the result of the deposition of silver onto the surface of the GNRs once the silver ions are reduced by ascorbate; this situation is confirmed by inductively coupled plasma mass spectrometry, which indicates that the ¹⁰⁹Ag/¹⁹⁷Au ratios are 0.046, 0.085, and 0.097 (RSD <2.9%) at pH 8.0, 9.0, and 10.0, respectively, from three consecutive measurements (20 data points were obtained in each measurement).²² The ratios of Ag to Au are in good agreement with those obtained by energy-dispersive X-ray (EDX) spectrometry (three consecutive measurements). A representative EDX spectrum is depicted in Figure 2E. The deposition of silver on GNRs explains why the values of the absorbance of the solutions at pH 9.0 and 10.0 (Figure 1) are much greater than that of the original solution. It has been known that the longitudinal plasmon absorption of GNRs shifts blue and is enhanced with silver coating, mainly because of the changes in dielectric function and overall aspect ratio, as well as the formation of the Au–Ag interface.^{20b,20c,23} We note that the Au–Ag core–shell NRs comprise >90% of the nanorods. At pH 9.0, most of the Au–Ag core–shell NRs possess dumbbell-shaped morphologies. The formation of the differently dumbbell-shaped Au–Ag core–shell NRs suggests that the {111} facet of the GNRs is more accessible to silver atoms than is the {110} facet, in which densely packed CTAB assemblies were formed.^{14b,24} We stress that our results are different from those described for the regular rodlike shapes obtained when using NH₂-OH to reduce silver on the surface of the GNRs in the absence of CTAB.²³ Table 1 summarizes the sizes, shapes, and surface plasmon absorptions of the as-prepared GNRs and the Au–Ag core–shell NRs; Chart 1 provides definitions of the descriptors L_1 , L_2 , D_1 , and D_2 . Both the length

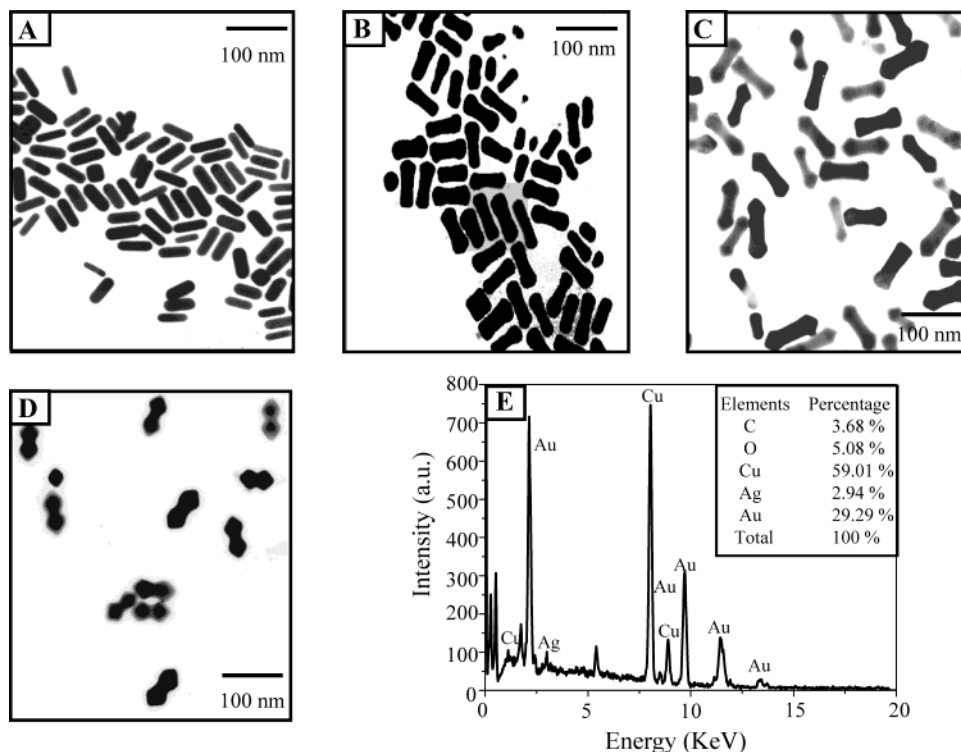
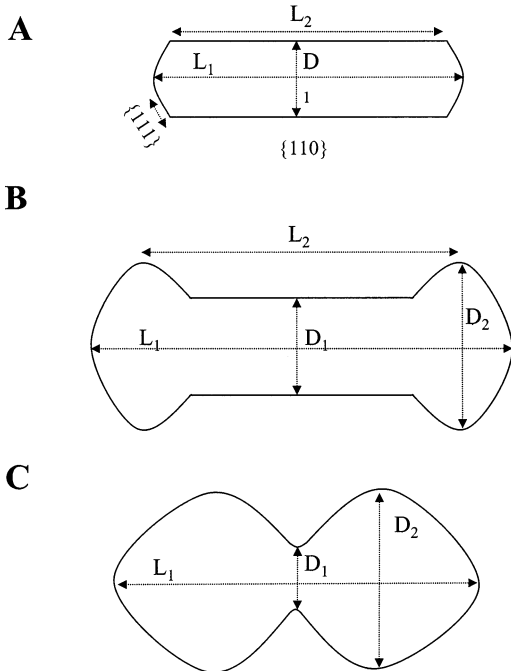


Figure 2. TEM images of the GNR solutions obtained at different values of pH: (A) pH 3.0, (B) pH 8.0, (C) pH 9.0, and (D) pH 10.0. A representative EDX spectrum of the GNR at pH 10.0 is depicted in (E). Scale bar = 100 nm. Other conditions are identical to those described in Figure 1.

Table 1. The Physical and Optical Properties of the GNRs and Au–Ag Core–Shell NRs^a

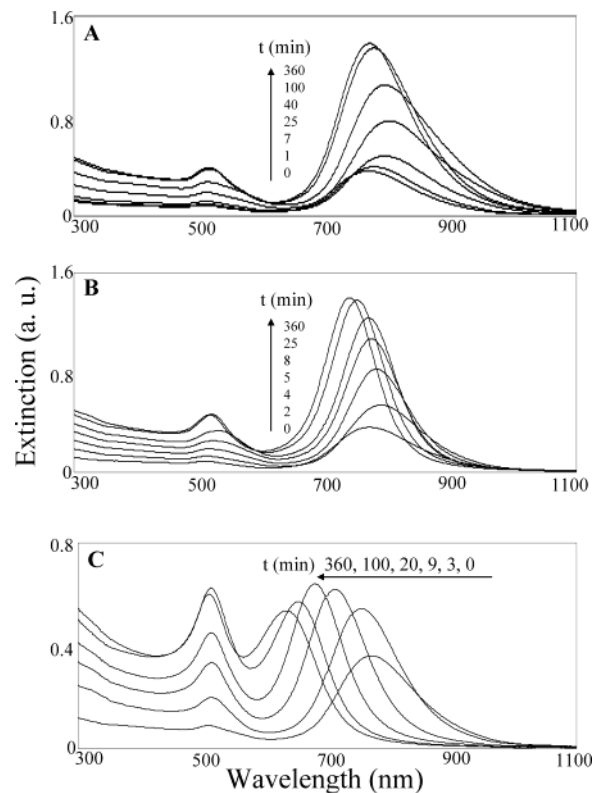
	L_1	L_2	D_1	D_2	L_1/D_1	L_1/D_2	λ_T (nm)	λ_L (nm)
GNRs	53 ± 4	43 ± 4	14 ± 3	14 ± 3	3.8	3.8	518	797
Au–Ag (pH 8.0)	56 ± 8	40 ± 8	15 ± 3	16 ± 4	3.7	3.5	517	781
Au–Ag (pH 9.0)	65 ± 8	36 ± 7	19 ± 4	24 ± 4	3.4	2.7	516	750
Au–Ag (pH 10.0)	58 ± 5	34 ± 5	19 ± 3	28 ± 2	3.1	2.1	515	637

^a The descriptors L_1 , L_2 , D_1 , and D_2 are defined in Scheme 1. The descriptors λ_T and λ_L represent the maximum wavelengths of the transverse and longitudinal plasmon absorbances, respectively.

Chart 1. The Model Structures of GNRs Listed in Table 1: (A) pH 8.0, (B) pH 9.0, and (C) pH 10.0

and diameter of the Au–Ag core–shell NRs increase, whereas the ratio $L_1:D_2$ decreases, as greater amounts of silver become deposited onto the surface of the GNRs at increasing values of pH. Since the $L_1:D_2$ ratio is similar to the aspect ratio, we expected that the longitudinal plasmon absorbance bands would shift toward the blue and the transverse absorption would shift toward the red upon increasing the pH.^{19,25} Surprisingly, we observe only the blue shift in the longitudinal plasmon absorption bands, but not a shift in the transverse plasmon absorbance bands, mainly because of the contribution of the absorbance of the Ag shell.^{20b,24} It is also important to note that the Au–Ag core–shell NRs prepared at both pH 8.0 and 9.0 display approximately 5-fold enhancements in their longitudinal plasmon absorbance relative to that of the GNRs.^{20a,20b,23} The intensities of both the transverse and longitudinal plasmon absorption bands are further enhanced as the concentration of AgNO_3 is increased.^{20b,23} The longitudinal surface plasmon absorbance shifts to shorter wavelengths upon increasing the concentration of silver ions, which indicates that the silver shell is thicker at higher concentrations of silver ions.^{20b,20c,23} A new absorption band appears at ca. 408 nm in the cases where AgNO_3 was used at concentrations >0.50 mM, which is due mainly to the formation of silver NPs; this situation is supported by the TEM image (not shown).

Figure 3 depicts the evolution with time of the formation of the differently dumbbell-shaped Au–Ag core–shell NRs. The rates of formation of the Au–Ag core–shell NRs at pH 8.0 and 9.0 slowed after 100 and 25 min, respectively. We attribute the faster rate that occurs at pH 9 to be due mainly to the increased concentration of ascorbate ions,

**Figure 3.** UV–vis absorption spectra displaying the time evolution of the formation of the Au–Ag core–shell NRs: (A) pH 8.0, (B) pH 9.0, and (C) pH 10.0. Other conditions identical to those described in Figure 1.

which possess greater reducing ability than does ascorbic acid. At pH 10.0, the longitudinal plasmon absorbance band undergoes a gradual blue shift and the transverse plasmon absorbance gradually increases during the course of the reaction (360 min). We believe that the longer reaction time needed at pH 10.0 is likely to be due to the slower rate of deposition as the Ag shell becomes thicker. The as-prepared dumbbell-shaped GNRs all are stable in glycine buffers (pH 3.0–10.0) for at least 3 months, indicating that glycine likely coated on their surface.

In summary, we describe an easy and reproducible method for preparing high-quality dumbbell-shaped bimetallic Au–Ag core–shell NRs. Silver ions are reduced effectively by ascorbate ions under alkaline conditions and become coated subsequently onto the surfaces of the GNRs. Because the coating of silver occurs anisotropically

(21) Srnova-Sloufova, I.; Lednický, F.; Gemperle, A.; Gemperlova, J. *Langmuir* **2000**, *16*, 9928–9935.

(22) Wrobel, K.; Sadi, B. B. M.; Wrobel, K.; Castillo, J. R.; Caruso, J. A. *Anal. Chem.* **2003**, *75*, 761–767.

(23) Ah, C. S.; Hong, S. D.; Jang, D.-J. *J. Phys. Chem. B* **2001**, *105*, 7871–7873.

(24) Wang, Z. L.; Gao, R. P.; Nikoobakht, B.; El-Sayed, M. A. *J. Phys. Chem. B* **2000**, *104*, 5417–5420.

(25) Link, S.; El-Sayed, M. A. *J. Phys. Chem. B* **1999**, *103*, 8410–8426.

on the surface of the GNRs in the presence of CTAB, the morphology of the Au–Ag core–shell NRs produced depends on the value of pH and on the concentration of AgNO₃. From our preliminary results, we note that this simple method may be extended to the synthesis of different Au–metal core–shell NRs merely by controlling the value of the pH and the nature and concentration of the buffer solution and reducing agents. It is worth noting that the Au–Ag core–shell NRs described herein possess stronger plasmon absorptions than do GNRs and, thus,

they have great potential for many applications, such as the detection of biomolecules and ions.^{6,26,27}

Acknowledgment. This work was supported by the National Science Council (NSC 93-2120-M-002-001) of the Republic of China.

LA048791W

(26) Hirsch, L. R.; Jackson, J. B.; Lee, A.; Halas, N. J.; West, J. L. *Anal. Chem.* **2003**, *75*, 2377–2381.

(27) Lee, T. M.-H.; Li, L.-L.; Hsing, I.-M. *Langmuir* **2003**, *19*, 4338–4343.